

# A Review and Modeling of Different Droop Control Based Methods for Battery State of the Charge Balancing in DC Microgrids

Niloofer Ghanbari<sup>1</sup>, M. Mobarrez<sup>2</sup>, and S. Bhattacharya<sup>1</sup>

<sup>1</sup>Department of Electrical and Computer Engineering  
North Carolina State University, Raleigh, NC, USA

<sup>2</sup>ABB Corporate Research Center, Raleigh, NC, USA

**Abstract**—Nowadays, DC microgrids by linking DC sources such as renewable resources directly to the DC loads and offering higher efficiency due to the elimination of conversion stages are gaining more and more popularity. In DC microgrids with renewable resources, there are stochastic behavior and uncertainties. Thus, energy storage use is unavoidable. Droop control as a well known method is used as the basis of the power sharing among different parallel voltage sources and battery energy storage systems (BESSs). In order to extend the lifetime of BESSs and avoid the overuse of a certain battery, the State of the Charge (SoC) of BESSs should be balanced. This paper presents a review on three different droop control based methods for balancing SoCs of different BESSs in DC microgrids. Moreover, the paper proposes a new droop control method for SoC balancing to overcome the drawbacks of the mentioned methods. The mathematical model of these different methods are derived using small signal state space modeling for a Photovoltaic (PV) grid-interactive DC microgrid consisting of two BESSs. Then, a comparison study has been performed for the mentioned four methods using MATLAB/Simulink.

**Index Terms**—DC microgrid, Droop Control Method, Battery Energy Storage System (BESSs), State of the Charge (SoC) Balancing

## I. INTRODUCTION

Department of Energy (DoE) defines microgrid as "a group of interconnected loads and distributed energy resources within clearly defined electrical boundaries that acts as a single controllable entity with respect to the grid. A microgrid can connect and disconnect from the grid to enable it to operate in both grid-connected or island-mode."

In existing AC PV microgrids, PV generates DC voltage, this DC voltage is inverted to AC through a grid-tied inverter and on the load side the AC voltage is converted to DC once again. This AC power system requires two energy conversion steps, DC/AC conversion at the PV side and AC/DC conversion at the DC load side. Renewable energy sources like solar and fuel cells generate DC power, on the other hand a large and increasing portion of loads use DC voltage internally. There is a possibility to eliminate the costly and inefficient power inverters and install a DC network linking DC loads to the DC sources- i.e., DC microgrid- [1]- [4]. PV and fuel cells are DC resources and they are connecting to the power grid by

DC/DC and DC/AC converters. DC/DC converters are mainly used to provide a controlled output voltage under different load variation [5].

BESSs are key elements of a DC microgrid due to the uncertainties in the nature of the renewable sources. Moreover, in order for obtaining a redundant system, there is need for multiple BESSs with power sharing capability [6].

When more than one BESS are utilized in a DC microgrid, some of them might be exposed to deep-discharging or overcharging if there is no control on the power sharing among them [6]. Therefore, it is necessary to design a controller that can dynamically change the power shared between the BESSs to keep their SoCs at the same level.

To achieve power sharing among BESSs, droop control methods have been proposed [7]. Droop control method is a well known method in DC microgrids, where the reference voltage of each source is calculated using its nominal output voltage, output current and a droop coefficient. The droop control methods can be modified to balance the SoCs besides the power sharing.

It is desirable that, in the discharging mode of operation, the BESS with higher SoC provides more power and accordingly, in the charging mode of operation, the BESS with lower SoC absorbs more power. To address this objective, some of the recent works dynamically change the droop coefficients of each BESS according to its SoC [4] - [12].

In [4], SoC balancing is achieved by comparing the SoC of each BESS with the average SoC of the batteries and have the BESSs with higher SoC to contribute more in discharging and the batteries with lower SoCs to contribute more in charging. There is another method for the SoC balancing which has been widely utilized in several literature [8] and [9]. In this method, the droop coefficient of a BESS is changed linearly according to its own SoC.

Another droop control based SoC balancing method is proposed in [11] to achieve SoC balancing of BESS with different capacities. The advantage of this method is that the batteries can have different capacities and their SoC will be balanced despite their different capacities, which cannot be obtained in other methods.

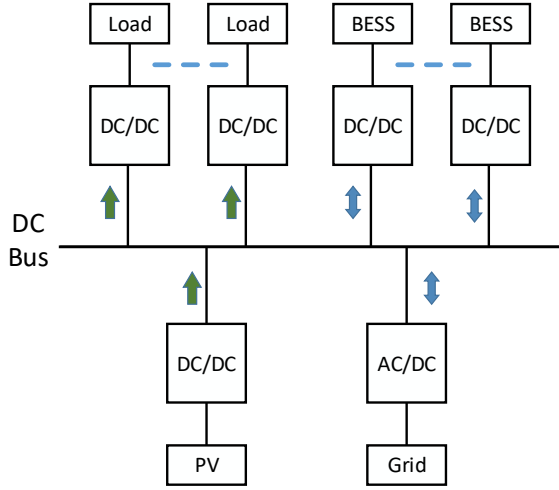


Fig. 1: Schematic diagram of a simple DC microgrid.

The paper is organized as following. In Section II, architecture and control of a typical DC microgrid utilizing droop control is discussed. Section III, describes different droop based control strategies and a new droop control method for SoC balancing is proposed to overcome the drawbacks of the other methods. In Section IV, state space models of different cases are derived and linearized using small signal method. Then in Section V, a comparison study has been performed for the mentioned four methods using MATLAB/Simulink. Finally, section VI concludes the overall paper.

## II. A TYPICAL DC MICROGRID

A typical PV DC microgrid consists of grid-tied converter, BESSs, PV arrays and loads connected to the common DC bus, as shown in Fig. 1.

Since the focus of this paper is on the control of BESSs, the rest of the system including PV, grid-tied converter and loads are considered as variable current sinks/sources and BESSs of the system regulate the DC bus voltage.

Block diagram of a BESSs and its three layers of control including: droop controller, voltage and current controllers are shown in Fig. 2. The primary controller, i.e., the voltage and current controllers, of each BESS is designed with the knowledge of its topology, switches, power source, and output capacitance such that it is stable under any external load fluctuations within the limits of its power rating. The secondary controller is responsible to handle energy management between BESSs and consists of droop control based SoC balancer followed by a SoC calculator which is responsible to monitor the SoC of BESSs and feed the SoC to the SoC balancer for modifying the droop coefficient. The procedure of designing the controllers has been discussed in details by the authors of this paper in [13].

The SoC of a battery is calculated based on its initial SoC, output current and capacity using the following equation

$$SoC_i = SoC_{i0} - \frac{1}{C_{ei}} \int I_i(t) dt \quad (1)$$

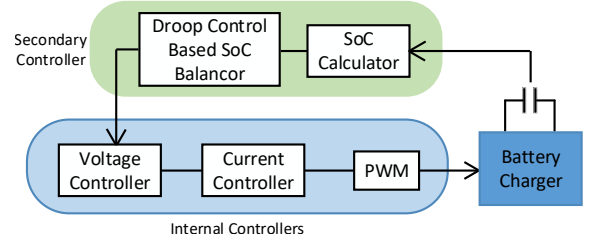


Fig. 2: Control block diagram of the battery charge controller.

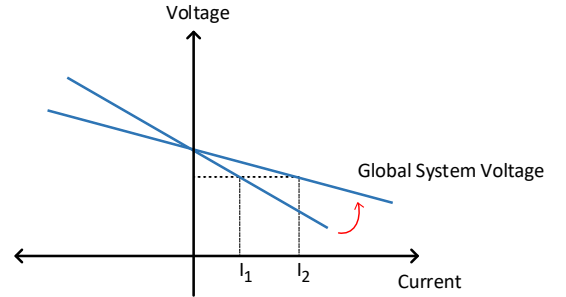


Fig. 3: Change of current due to the change of droop coefficient.

where,  $SoC_{i0}$  is the initial SoC of  $i^{th}$  battery,  $C_{ei}$  is the capacity of the battery in  $As$  and  $I_i(t)$  is the output current of the battery.

The calculated SoC from Eq.1 can be used to modify the droop coefficient of the battery and adjust its output power. Fig. 3 shows the I-V characteristic of a BESS with different droop coefficient. This figure shows that how the output current of the battery varies with change in its droop coefficient. Therefore, by modifying the droop coefficient of each BESS, its contribution in voltage regulation can be controlled. For instance, by decreasing the droop coefficient, the BESS output current increases and discharges faster consequently.

Hence, the droop coefficients of paralleled BESSs shall be modified according to their SoCs. The control objective of this modification is to keep the SoC of all BESSs at the same level and avoid deep discharging and over charging of a particular battery. This is achieved by forcing the BESSs with higher SoC contributes more in discharging and the BESSs with lower SoC contributes more in charging.

There are different methods for adjusting the droop coefficients of BESSs based on their SoCs. In the following section, three possible methods for SoC balancing is discussed and a novel control method is proposed to overcome the drawbacks of the other methods.

## III. POSSIBLE SOC BALANCING METHODS

In order to balance the SoCs of BESSs in a DC microgrid, the BESSs that have higher SoC should discharge faster and charge slower than the others. In this paper, it is assumed that the paralleled BESSs are utilizing voltage droop control for power sharing. And the basis of all the SoC balancing methods that will be discussed in the following, is updating the droop coefficient of the BESSs.

**Method 1:** In this method, the droop coefficient is modified as following [4]

$$\begin{cases} R_{d_i}^{new} = \frac{R_{d_i}}{\beta_i} & \text{Discharging} \\ R_{d_i}^{new} = R_{d_i}\beta_i & \text{Charging} \end{cases} \quad (2)$$

where,  $R_{d_i}^{new}$  is the modified droop coefficient,  $R_{d_i}$  is the initial droop coefficient and  $\beta_i$  is defined as

$$\beta_i = \frac{SoC_i}{\frac{1}{n} \sum_{k=1}^n SoC_k} \quad (3)$$

where,  $n$  is the total number of BESSs in the system.

In this equation,  $SoC_i$  corresponds to SoC of  $i^{th}$  battery and is changing with time as following

$$SoC_i = SoC_i(0) - \frac{1}{C_e} \int i_i(t) dt \quad (4)$$

It can be seen from Eq. 2, that if the SoC of  $i^{th}$  battery is greater than the average of SoC of all BESSs,  $\beta_i$  is greater than 1 and if the SoC is less than the average of SoCs,  $\beta_i$  is less than 1. Thus, the BESSs with higher SoC with respect to the average would have smaller droop coefficient which results in higher discharging current. The same analysis is valid for the case when the batteries are charging.

**Method 2:** In order to achieve SoC balancing of BESSs with different capacities, the droop coefficient can be modified as following [11]

$$\begin{cases} R_d^{new} = \frac{R_d}{C_{ei}}(1 - K_{SoC}SoC_i) & \text{Discharging} \\ R_d^{new} = \frac{R_d}{C_{ei}}(K_{SoC}SoC_i - 1) & \text{Charging} \end{cases} \quad (5)$$

where,  $K_{SoC}$  is a factor that can be selected arbitrary. From the above equation, it can be seen that the objective of forcing the BESSs with higher SoC to discharge at the higher rate, is achieved by increasing the corresponding droop coefficient and reducing the output current.

This method unlike the other methods, takes the capacity of BESSs into consideration as well as the SoC itself. According to Eq. 5, the BESS with higher capacity discharges at a higher rate and charges at a lower rate than the others.

**Method 3:** In this case, the droop coefficient is divided by the SoC of BESSs for the discharging operation mode and multiplied by the SoC of BESSs for the charging operation mode. This method is very common and used in many literature [8] - [9]. The droop equations for the discharging and charging operation modes are as follows, respectively:

$$\begin{cases} R_d^{new} = \frac{R_{d_i}}{SoC_i} & \text{Discharging} \\ R_d^{new} = R_{d_i}SoC_i & \text{Charging} \end{cases} \quad (6)$$

The advantage of using this method is that each BESS's droop coefficient relates to its own characteristics,  $R_{d_i}$  and  $SoC_i$ . In other words, the droop controller is not dependent on the SoC of other BESSs and hence there is no need for communication between batteries or central controller for broadcasting the information of batteries.

This method increases (decreases) the droop coefficients of all the BESSs for balancing the SoCs in discharging (charging)

operation mode. Therefore, there is a possibility that the DC bus voltage doesn't remain in the desired range. One way to address this issue is to limit the voltage variations by limiting the currents of BESSs. However, the battery converters are not fully utilized in this method. The previous method also suffers from this drawback.

**Proposed Method:** To address the discussed drawback, we propose a droop control based SoC balancing. In this method, the new droop coefficient  $R_{d_i}^{new}$  is calculated using the deviation of its own SoC from the average SoCs of other BESSs.

The following equation shows how the droop coefficient of each BESS is calculated with the proposed method.

$$\begin{cases} R_{d_i}^{new} = (1 - (SoC_i - \frac{\sum_{k \neq i} SoC_k}{n}))R_{d_i} & \text{Discharging} \\ R_{d_i}^{new} = (1 - (\frac{\sum_{k \neq i} SoC_k}{n} - SoC_i))R_{d_i} & \text{Charging} \end{cases} \quad (7)$$

Eq. 7 shows that the droop coefficient of a BESS can be decreased or increased in both discharging and charging mode, depending on its SoC's deviation from the average SoC of other BESSs. This modification will help in keeping the bus voltage in the desired range while increasing the battery converter utilization.

The proposed method can be modified to reflect the capacities of BESSs. The droop coefficient for different BESSs having different capacities shall be normalized with respect to their capacities. Thus, the new droop coefficient can be written as

$$R_{d_i}^* = \frac{R_{d_i}}{C_{e_i}} \quad (8)$$

Therefore, the proposed method can become applicable to a system consisting of BESSs with different capacities with minor modification as following

$$\begin{cases} R_{d_i}^{new} = (1 - (SoC_i - \frac{\sum_{k \neq i} SoC_k}{n})) \frac{R_{d_i}}{C_{e_i}} & \text{Discharging} \\ R_{d_i}^{new} = (1 - (\frac{\sum_{k \neq i} SoC_k}{n} - SoC_i)) \frac{R_{d_i}}{C_{e_i}} & \text{Charging} \end{cases} \quad (9)$$

#### IV. STATE SPACE MODELING OF A DC MICROGRID

In this section, state space modeling method is used to model the DC microgrid. The state space description is a well known method for describing a system in terms of mathematical model. This mathematical model can be simulated and the behavior of the states of the system can be observed.

In order to obtain the state space model, different states of the system should be defined. In a typical DC microgrid with multiple voltage sources as parallel, the states can be defined for the voltage sources of the system due to the dynamics that exist in the converter and controllers.

In the given DC microgrid, the BESSs are the only voltage sources of the system. Thus, the state variables shall be defined for BESSs with their controllers. Then, the state space models of all BESSs shall be combined together to form the mathematical model of the DC microgrid. In this paper, for simplicity and without loss of generality, we consider just two BESSs as the voltage sources of the system.

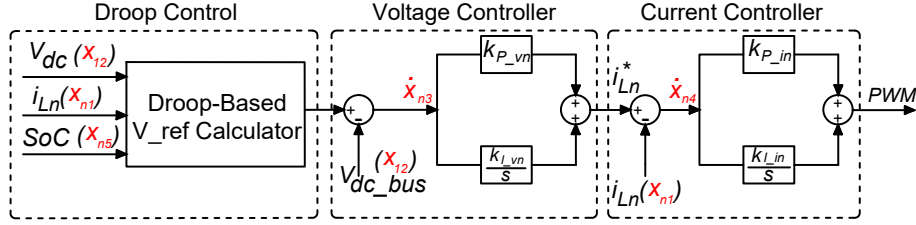


Fig. 4: Block diagram and state definition for a BESS with its controllers.

TABLE I: States definition of the first BESS as a voltage source converter.

State Variable	Description
$x_{11}$	Inductor Current
$x_{12}$	Capacitor Voltage
$x_{13}$	Output of the Voltage Controller Intergrator
$x_{14}$	Output of the Current Controller Intergrator
$x_{15}$	SoC of BESS

Fig. 4 shows the control block diagram of a BESS with its controllers: droop controller, voltage controller, and current controller. For this converter and set of controllers, the state variables are defined in Table I. In this paper all the battery DC-DC converters are considered as bidirectional buck converters.

The defined states are related to the first battery. For the second battery, the states are defined the same, but their first indices should be changed to 2.

It should be noted that when two BESSs are connected to the DC bus as parallel, their output voltages should be the same. Hence, for the second BESSs, the state corresponds to the capacitor voltage is removed.

In the power electronics systems, the inductor currents and capacitor voltages are considered as the state variables of the system. In this paper, as the SoCs of batteries change dynamically, they are considered as state variables and can be defined as

$$x_{15} = SoC_1 = SoC_1(0) - \frac{1}{C_{e1}} \int i_1(t) dt \quad (10)$$

By replacing  $i_1(t)$  with  $x_{11}$  and taking derivatives, we have

$$SoC_1 = x_{15} = \frac{-1}{C_{e1}} x_{11} \quad (11)$$

Using the defined state variables, the mathematical model of the DC microgrid for different droop control based SoC balancing methods presented in the previous section can be obtained. The detailed model derivation are explained in the following.

**Method 1:** From Fig. 4,  $x_{13}$  can be written as

$$x_{13} = V_{nom} - R_{d1}^{new} x_{11} - x_{12} \quad (12)$$

Then, the droop coefficient is replaced with the modified one presented in Eq. 2.

$$x_{13} = V_{nom} - \frac{R_{d1}}{\beta_1} x_{11} - x_{12} \quad (13)$$

For a system with two batteries,  $\beta_1$  can be written as

$$\beta_1 = \frac{SoC_1}{\frac{1}{2}(SoC_1 + SoC_2)} \quad (14)$$

Then,

$$\frac{R_{d1}}{\beta_1} = \frac{R_{d1}}{2} \left(1 + \frac{SoC_2}{SoC_1}\right) \quad (15)$$

Combining Eq. 13 and Eq. 15, we have

$$x_{13} = V_{nom} - \frac{R_{d1}}{2} x_{11} - x_{12} - \frac{R_{d1}}{2} \frac{x_{25}}{x_{15}} x_{11} \quad (16)$$

To model the nonlinearity of Eq. 16 into standard model, the small signal model obtained considering operating point as  $x_{11}(0)$ ,  $x_{15}(0)$  and  $x_{25}(0)$ .

$$\frac{x_{25}}{x_{15}} x_{11} = \frac{x_{25}(0)}{x_{15}(0)} x_{11} + \frac{x_{11}(0)}{x_{15}(0)} x_{25} - \frac{x_{11}(0)x_{25}(0)}{x_{15}^2(0)} x_{15} \quad (17)$$

From Eq. 17 and Eq. 16,  $x_{13}$  can be written as

$$x_{13} = V_{nom} - \frac{R_{d1}}{2} (1 + \mu_{12}) x_{11} - x_{12} - \frac{R_{d1} \mu_{13}}{2} x_{25} + \frac{R_{d1} \mu_{14}}{2} x_{15} \quad (18)$$

where,

$$\mu_{12} = \frac{x_{25}(0)}{x_{15}(0)} \quad \mu_{13} = \frac{x_{11}(0)}{x_{15}(0)} \quad \mu_{14} = \frac{x_{11}(0)x_{25}(0)}{x_{15}^2(0)} \quad (19)$$

The other state variables can be defined in the same manner to obtain the model of a single converter. The detailed derivation and modeling of a single converter in microgrids were discussed by the authors of this paper in [13].

**Method 2:** From Fig. 4,  $x_{13}$  can be written as

$$\begin{aligned} x_{13} &= V_{nom} - R'_{d1} (1 - K x_{15}) x_{11} - x_{12} \\ &= V_{nom} - R'_{d1} x_{11} + K R'_{d1} x_{11} x_{15} - x_{12} \end{aligned}$$

where,  $R'_{d1} = \frac{R_{d1}}{C_{e1}}$  and  $K = K_{SoC}$ .

The term  $K R'_{d1} x_{11} x_{15}$  is nonlinear and needs to be linearized using small signal analysis as the following

$$K R'_{d1} x_{11} x_{15} = K R'_{d1} x_{11}(0) x_{15} + K R'_{d1} x_{15}(0) x_{11} \quad (20)$$

Thus, the equation for  $x_{13}$  can be rewritten as

$$x_{13} = V_{nom} - (R_{d1} - K R_{d1} x_{15}(0)) x_{11} - x_{12} + K R_{d1} x_{11}(0) x_{15} \quad (21)$$

By taking the same procedure as in method 1, the state space model for a single BESS can be found.

This state space model can be utilized for the other BESSs of the system. It should be noted that since in this case the droop coefficient of each BESS is modified based on its own SoC, the state space model of two BESSs are completely independent from each other. Therefore, the state space model of a system with two BESSs is a block diagonal matrix containing the state space matrix of BESS1 and BESS2 on its diagonal elements.

**Method 3:** Similar to the previous methods,  $x_{13}$  can be written as

$$\dot{x}_{13} = V_{nom} - \frac{R_{d1}}{x_{15}} x_{11} - x_{12} \quad (22)$$

In the above equation, second term contains two state variables and is nonlinear. Thus, it needs to be linearized using the same procedure as the previous cases.

$$-\frac{R_{d1}}{x_{15}} x_{11} = -\frac{R_{d1}}{x_{15}(0)} x_{11} + \frac{R_{d1} x_{11}(0)}{x_{15}^2(0)} x_{15} \quad (23)$$

By replacing this linearized term in Eq. 22, we have

$$\dot{x}_{13} = V_{nom} - R_{d1} \frac{1}{x_{15}(0)} x_{11} - x_{12} + \frac{R_{d1} x_{11}(0)}{x_{15}^2(0)} x_{15} \quad (24)$$

This state space model can be utilized for the other BESSs of the system. Since the droop coefficient of each BESS is modified based on its own SoC, the state space model of a system with two BESSs is a block diagonal matrix containing the state space matrix of BESS1 and BESS2 on its diagonal elements.

**Proposed Method:** The same as the previous methods,  $x_{13}$  is written as

$$\dot{x}_{13} = V_{nom} - R_{d1}(1 - x_{15} + x_{25})x_{11} - x_{12} \quad (25)$$

The second term is nonlinear. Thus, it needs to be linearized using small signal analysis.

$$(1 - x_{15} + x_{25})x_{11} = x_{11} - x_{15}(0)x_{11} + x_{25}(0)x_{11} - x_{11}(0)x_{15} + x_{11}(0)x_{25}$$

By replacing the linearized term in the previous equation, we have

$$\dot{x}_{13} = V_{nom} - R_{d1}(1 - x_{15}(0) + x_{25}(0))x_{11} - x_{12} + R_{d1}x_{11}(0)x_{15} - R_{d1}x_{11}(0)x_{25}$$

Using the same procedure as method 1, state space model of the DC microgrid containing two BESSs can be derived. This model can be found in the appendix.

## V. SIMULATION RESULTS

In order to test the feasibility and effectiveness of the derived mathematical models of the DC microgrid, the obtained state space model of the system consisting of two BESSs are simulated in MATLAB/Simulink. The simulation parameters of the DC microgrid are listed in Table II. The following shows the SoC balancing results for all of the discussed methods.

TABLE II: Specifications of the simulated DC microgrid.

Parameter	Description	Amount
$L_1, L_2$	Inductance of battery converter output filter	5 mH
$C_1, C_2$	Capacitance of battery converter output filter	$500\mu F$
$R_{d1}, R_{d2}$	Voltage Droop coefficients of the battery converters	0.11
$V_{nom}$	Output nominal voltage of the converters	380VDC
$G_V(s)$	Transfer function of converters voltage controllers	$0.25 + \frac{2}{s}$
$G_I(s)$	Transfer function of converters current controllers	$2.5 + \frac{5}{s}$
$P_{load}$	Load power	30kW
$C_{e1}, C_{e2}$	Capacity of the BESSs	10000 As

Fig. 5 and 6 show how the SoC balancing is achieved using discussed balancing methods in the system with two BESSs with different initial SoCs in charging and discharging operation mode, respectively.

As it can be seen in this figure, the battery with higher SoC contributes more in discharging and less in charging. Similarly, the battery with lower SoC contributes less in discharging and more in charging. All of the mentioned methods result in convergence of BESSs' SoCs. However, the convergence speed varies from one method to another method.

In order to compare the convergence speed of the discussed methods, initial SoCs of BESSs are considered 0.6 and 0.4, respectively with capacity of 10000As for all BESSs. The time of convergence of SoCs for different methods are shown in Table III. It can be seen from this table that the proposed method has highest speed of convergence among the other presented methods.

The second important difference is the need for communication and ease of implementation. Some methods require central controller and communication network between the controller and BESSs. While other methods can balance the SoCs by measuring the local quantities (distributed controllers).

Another important fact that shall be considered and discussed is the amount of voltage variation. When there is no droop coefficient modification based on SoC balancing, the voltage drops from the nominal voltage according to the droop equation and will be  $R_d I = \Delta V$ . When the droop coefficients change according to the SoCs of batteries, the amount of currents BESSs produce or absorb are being changed. Thus, the amount of voltage variation will be changed accordingly. The amount of voltage variation added to the system by the droop control modification is summarized in Table III for different methods.

The other difference between the discussed methods is the applicability to the BESSs with different capacities. As it was mentioned in the previous sections, in method 2 and 4, the capacities of BESSs are considered in the modified droop coefficients of batteries. Therefore, it is applicable in a DC microgrid consisting of BESSs with different capacities.

TABLE III: Comparison of different methods considering specifications in Table I.

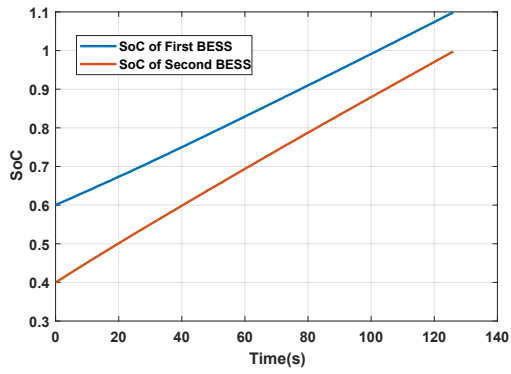
Method	Method 1	Method 2	Method 3	Method 4
Required time for SoC balancing	T	1.5T	1.1T	0.9T
Ease of implementation	Requires central controller and communication network between BESSs	Requires local measurements (distributed controller)	Requires local measurements (distributed controller)	Requires central controller and communication network between BESSs
Additional voltage variation				
Discharging operation mode:	0	$0.8\Delta V$	$4.16\Delta V$	0
Charging operation mode:	0	$0.6\Delta V$	$1\Delta V$	0
Applicability to the BESSs with different capacities	No	Yes	No	Yes

## VI. CONCLUSION

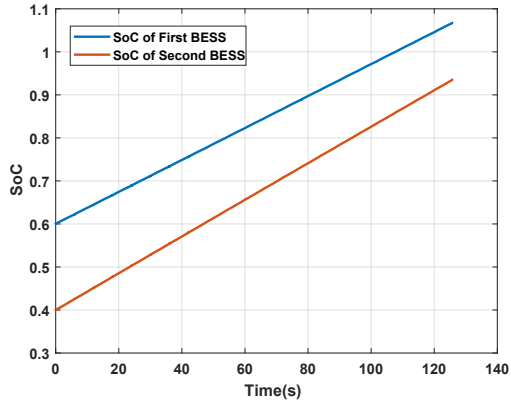
To extend the lifetime of BESSs and avoid the overuse of a certain battery in DC microgrids, the SoC of BESSs should be balanced. This paper presents a review on three different droop control based methods for balancing SoCs of different BESSs in DC microgrids. Moreover, the paper proposes a new droop control method for SoC balancing to overcome the drawbacks of the mentioned methods. The mathematical model of these different methods are derived using small signal state space modeling for a Photovoltaic (PV) grid-interactive DC microgrid consisting of two BESSs. Then, a comparison study has been performed for the mentioned four methods using MATLAB/Simulink. Moreover, these methods are compared in terms of required time for SoC balancing, ease of implementation, additional voltage variation, and applicability to the BESSs with different capacities.

## REFERENCES

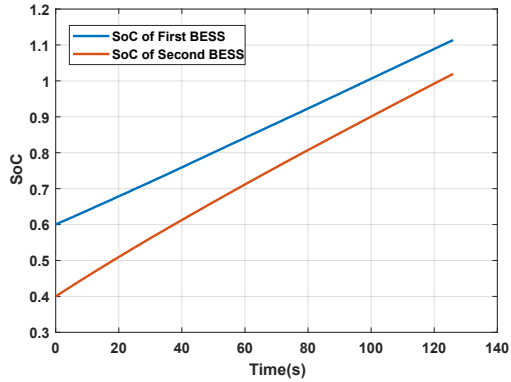
- [1] Dragicevic, T., Guerrero, J.M., Vasquez, J.C., and Skrlec, D., "Supervisory Control of an Adaptive-Droop Regulated DC Microgrid With Battery Management Capability", IEEE Transactions on Power Electronics, vol.29, no.2, pp.695-706, Feb. 2014.
- [2] Kakigano, H., Miura, Y., and Ise, T., "Low-Voltage Bipolar-Type DC Microgrid for Super High Quality Distribution", IEEE Transactions on Power Electronics, vol.25, no.12, pp.3066-3075, Dec. 2010.
- [3] J. M. Guerrero, P. C. Loh, T. L. Lee, and M. Chandorkar, "Advanced control architectures for intelligent microgrids - Part II: Power quality, energy storage, and ac/dc microgrids", IEEE Transaction on Industrial Electronics, vol. 60, no. 4, pp. 1263-1270, Apr. 2013.
- [4] N. Ghanbari, M. Mobarrez and S. Bhattacharya, "Modeling and Stability Analysis of a DC Microgrid Employing Distributed Control Algorithm", IEEE 9th International Symposium on Power Electronics for Distributed Generation Systems (PEDG), Charlotte, NC, USA, Jun. 2018.
- [5] P. M. Shabestari, G. B. Gharehpetian, G. H. Riahy, and S. Mortazavian, "Voltage controllers for DC-DC boost converters in discontinuous current mode," International Energy and Sustainability Conference (IESC), Farmingdale, NY, 2015, pp. 1-7.
- [6] C. Li, T. Dragicevic, N. L. Diaz, J. C. Vasquez, and J. M. Guerrero, "Voltage Scheduling Droop Control for State-of-Charge Balance of Distributed Energy Storage in DC Microgrids", IEEE International Energy Conference (ENERGYCON), Cavtat Croatia, May 2014.
- [7] B.T. Irving, and M.M. Jovanovic, "Analysis, design, and performance evaluation of droop current-sharing method", Applied Power Electronics Conference and Exposition (APEC), Los Angeles USA, Feb. 2000.
- [8] N. C. Sahoo, S. Mohapatra, and M. K. Senapati, "A SoC Based Voltage Control Strategy for DC Microgrid", Electrical Power and Energy Conference (EPEC), ON Canada, Oct 2015.
- [9] B. M. Han, "Battery SoC-based DC Output Voltage Control of BESS in Stand-alone DC Microgrid", Region 10 Conference (TENCON), Singapore, Nov. 2016.
- [10] R. Hu, and W. W. Weaver, "Dc Microgrid Droop Control Based on Battery State of Charge Balancing", Power and Energy Conference at Illinois (PECI), IL USA, Feb 2016.
- [11] A. J. Jones, and W. W. Weaver, "Optimal Droop Surface Control of Dc Microgrids Based on Battery State of Charge", Energy Conversion Congress and Exposition (ECCE), WA USA, Sep 2016.
- [12] Q. Wu, R. Guan, X. Sun, Y. Wang, and X. Li, "SoC Balancing Strategy for Multiple Energy Storage Units with Different Capacities in Islanded Microgrids Based on Droop Control", IEEE Journal of Emerging and Selected Topics in Power Electronics, vol. PP, no. 99, pp. 1-1, Jan. 2018
- [13] M. Mobarrez, N. Ghanbari, and S. Bhattacharya, "Control Hardware-in-the-Loop Demonstration of a Building-Scale DC Microgrid Utilizing Distributed Control Algorithm", IEEE PES General Meeting, Oregon USA, Sep. 2018



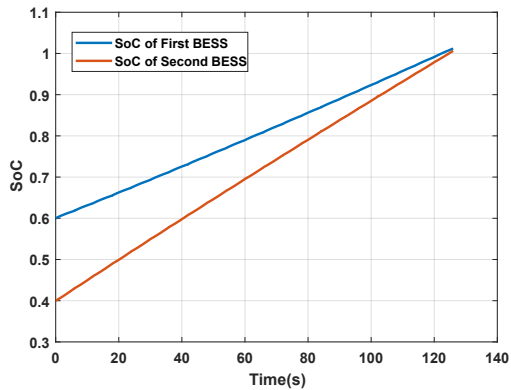
(a) Method 1



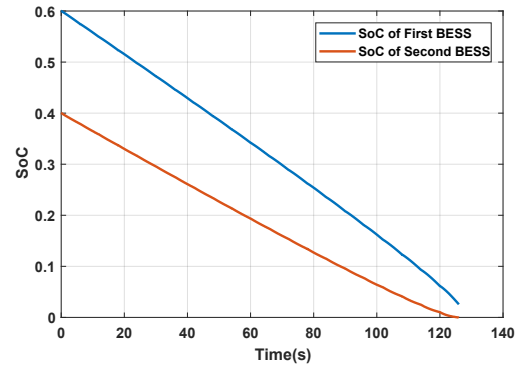
(b) Method 2



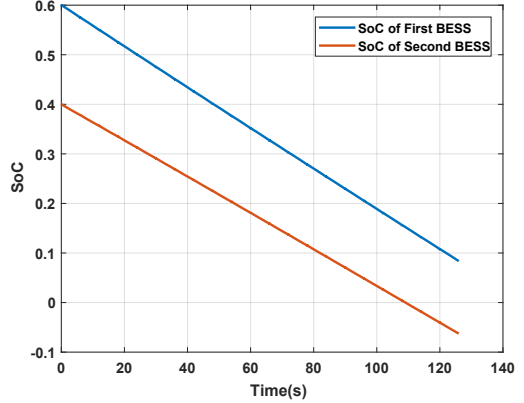
(c) Method 3



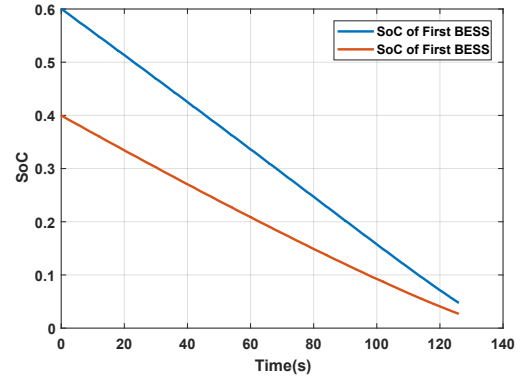
(d) Method 4



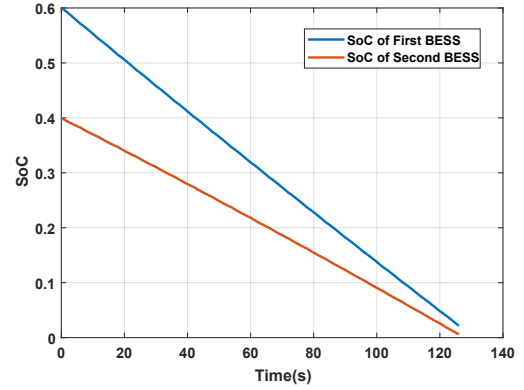
(a) Method 1



(b) Method 2



(c) Method 3



(d) Method 4

Fig. 5: SoCs of BESSs in the charging mode of operation.

Fig. 6: SoCs of BESSs in the discharging mode of operation.

VII. APPENDIX

Proposed Method:

$$\begin{bmatrix} \dot{x}_{11} \\ \dot{x}_{12} \\ \dot{x}_{13} \\ \dot{x}_{14} \\ \dot{x}_{15} \\ \dot{x}_{21} \\ \dot{x}_{23} \\ \dot{x}_{24} \\ \dot{x}_{25} \end{bmatrix} = \begin{bmatrix} a_{11} & a_{12} & a_{13} & a_{14} & a_{15} & 0 & 0 & 0 & a_{19} \\ a_{21} & a_{22} & 0 & 0 & 0 & a_{26} & 0 & 0 & 0 \\ a_{31} & -1 & 0 & 0 & a_{35} & 0 & 0 & 0 & a_{39} \\ a_{41} & a_{42} & a_{43} & 0 & a_{45} & 0 & 0 & 0 & a_{49} \\ \frac{-1}{C_{e1}} & 0 & 0 & 0 & 0 & 0 & 0 & 0 & 0 \\ 0 & a_{62} & 0 & 0 & a_{65} & a_{66} & a_{67} & a_{68} & a_{69} \\ 0 & -1 & 0 & 0 & a_{75} & a_{76} & 0 & 0 & a_{79} \\ 0 & a_{82} & 0 & 0 & a_{85} & a_{86} & a_{87} & a_{88} & a_{89} \\ 0 & 0 & 0 & 0 & 0 & \frac{-1}{C_{e2}} & 0 & 0 & 0 \end{bmatrix} \begin{bmatrix} x_{11} \\ x_{12} \\ x_{13} \\ x_{14} \\ x_{15} \\ x_{21} \\ x_{23} \\ x_{24} \\ x_{25} \end{bmatrix} + \begin{bmatrix} \frac{k_{P_{i1}}k_{P_{v1}}}{L_1} \\ 0 \\ 1 \\ k_{P_{v1}} \\ 0 \\ \frac{k_{P_{i2}}k_{P_{v2}}}{L_2} \\ 1 \\ k_{P_{v2}} \\ 0 \end{bmatrix} V_{nom} \quad (26)$$

$$a_{11} = \frac{-k_{P_{i1}} - k_{P_{i1}}k_{P_{v1}}R_{d1}(1 - x_{15}(0) + x_{25}(0))}{L_1}$$

$$a_{13} = \frac{k_{P_{i1}}k_{I_{v1}}}{L_1}$$

$$a_{15} = R_{d1}x_{11}(0)\frac{k_{P_{i1}}k_{P_{v1}}}{L_1}$$

$$a_{21} = \frac{1}{C_1 + C_2}$$

$$a_{26} = \frac{1}{C_1 + C_2}$$

$$a_{35} = R_{d1}x_{11}(0)$$

$$a_{41} = -1 - k_{P_{v1}}R_{d1}(1 - x_{15}(0) + x_{25}(0))$$

$$a_{43} = k_{I_{v1}}$$

$$a_{49} = -k_{P_{v1}}R_{d1}x_{11}(0)$$

$$a_{65} = R_{d2}x_{21}(0)\frac{-k_{P_{i2}}k_{P_{v2}}}{L_2}$$

$$a_{67} = \frac{-k_{P_{i2}}k_{P_{v2}}}{L_2}$$

$$a_{69} = R_{d2}x_{21}(0)\frac{k_{P_{i2}}k_{P_{v2}}}{L_2}$$

$$a_{76} = -R_{d2}(1 - x_{25}(0) + x_{15}(0))$$

$$a_{82} = -k_{P_{v2}}$$

$$a_{86} = -1 - k_{P_{v2}}R_{d2}(1 - x_{25}(0) + x_{15}(0))$$

$$a_{89} = k_{P_{v2}}R_{d2}x_{21}(0)$$

$$a_{12} = \frac{-k_{P_{i1}}k_{P_{v1}}}{L_1}$$

$$a_{14} = \frac{k_{I_{i1}}}{L_1}$$

$$a_{19} = R_{d1}x_{11}(0)\frac{-k_{P_{i1}}k_{P_{v1}}}{L_1}$$

$$a_{22} = \frac{-1}{R(C_1 + C_2)}$$

$$a_{31} = -R_{d1}(1 - x_{15}(0) + x_{25}(0))$$

$$a_{39} = -R_{d1}x_{11}(0)$$

$$a_{42} = -k_{P_{v1}}$$

$$a_{45} = k_{P_{v1}}R_{d1}x_{11}(0)$$

$$a_{62} = \frac{-k_{P_{i2}}k_{P_{v2}}}{L_2}$$

$$a_{66} = \frac{-k_{P_{i2}} - k_{P_{i2}}k_{P_{v2}}R_{d1}(1 - x_{15}(0) + x_{25}(0))}{L_2}$$

$$a_{68} = \frac{k_{I_{i2}}}{L_2}$$

$$a_{75} = -R_{d2}x_{21}(0)$$

$$a_{79} = R_{d2}x_{21}(0)$$

$$a_{85} = -k_{P_{v2}}R_{d2}x_{21}(0)$$

$$a_{87} = k_{I_{v2}}$$